## Supplemental Information

# Hidden role of intermolecular proton transfer in the anomalously diffuse vibrational spectrum of a trapped hydronium ion

Stephanie M. Craig,[a] Fabian S. Menges,[a] Chinh H. Duong,[a] Joanna K. Denton,[a] Lindsey R. Madison,[b] Anne B. McCoy[b] and Mark A. Johnson[a,*]

[a]Sterling Chemistry Laboratory, Yale University, New Haven, CT 06525, USA

[b]Department of Chemistry, University of Washington, Seattle, Washington 98195, USA

*M. A. Johnson. Tel: +1 203 432 5226, Email: mark.johnson@yale.edu

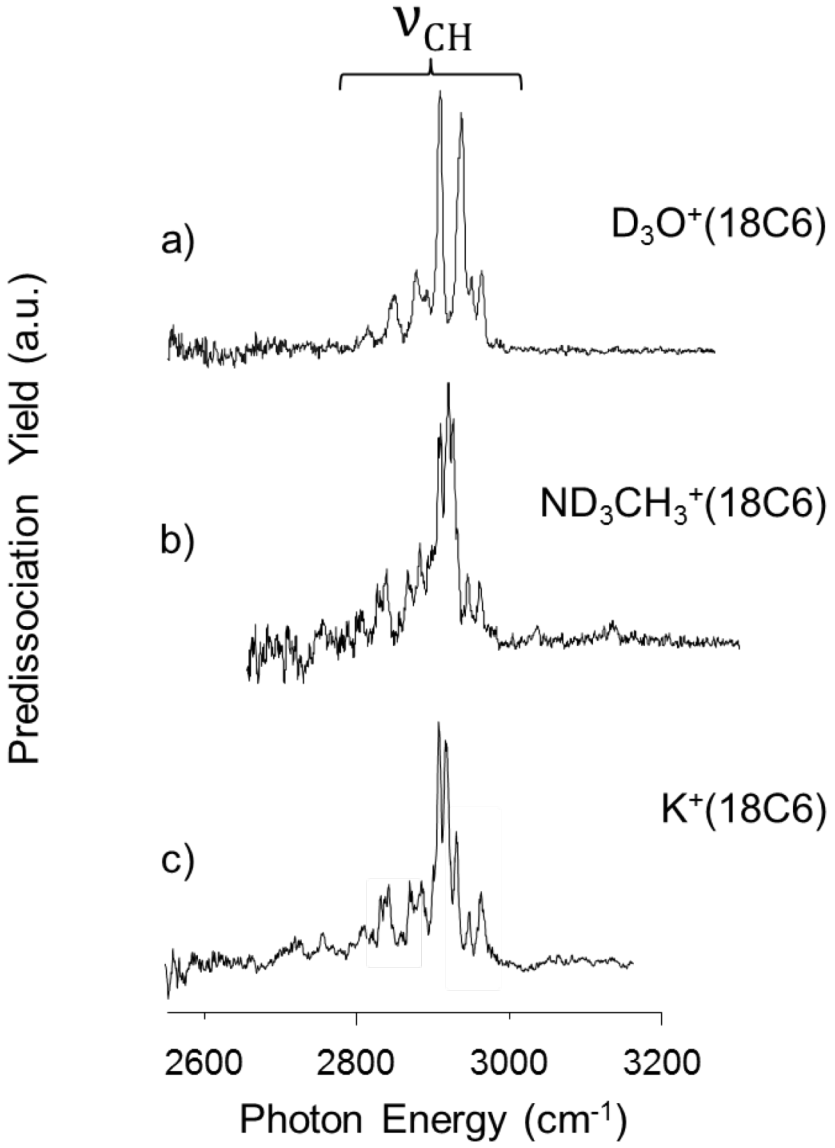


**Figure S1.** Vibrational predissociation spectra of a) $D_3O^+(18C6)\cdot D_2$, b) $ND_3CH_3^+(18C6)\cdot D_2$, and c) $K^+(18C6)\cdot D_2$ in the CH stretching region where the guest has been deuterated in order to isolate the CH stretches of the 18C6. Noteworthy is the further splitting of the intense doublet upon the uptake of $D_3O^+$.

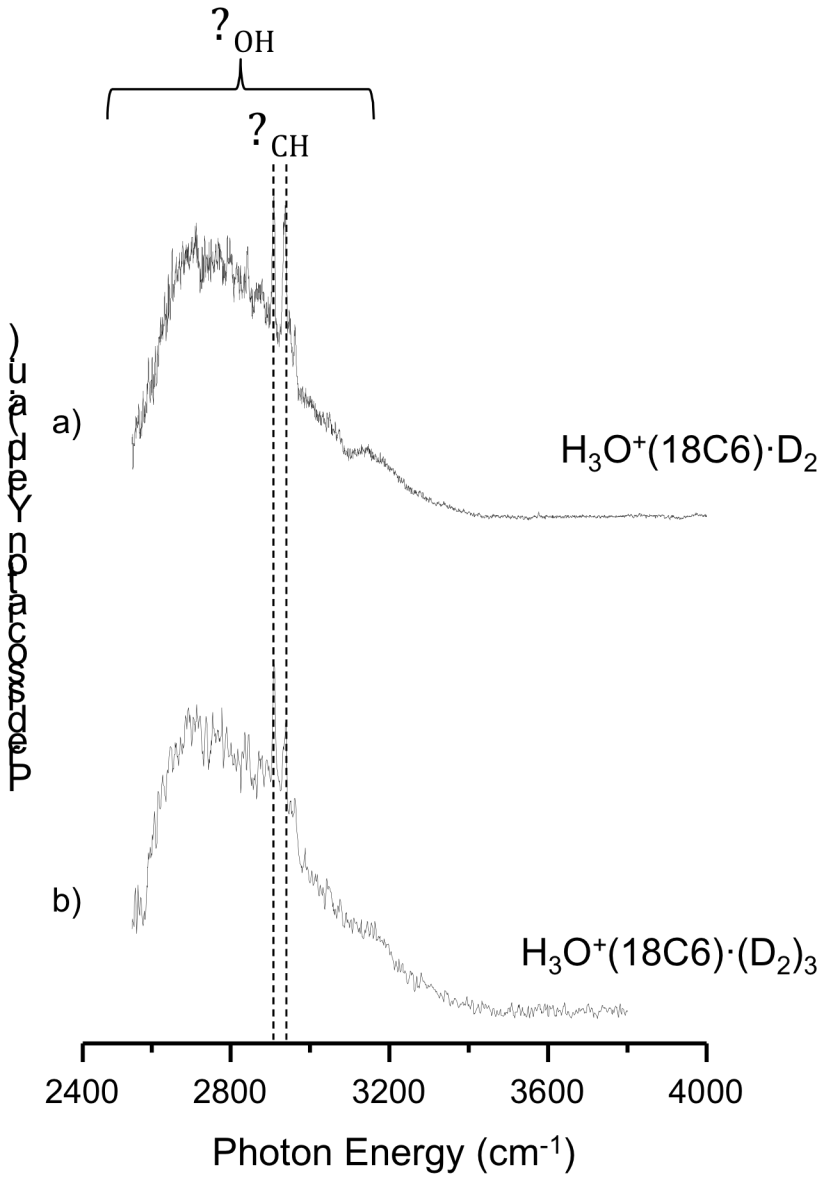


**Figure S2.** Tag dependence studies of $H_3O^+$(18C6) show that the breadth of the OH stretching region does not come from the presence or number of $D_2$ tags in the system, where a) is the predissociation spectrum for one $D_2$ tag and b) shows three $D_2$ tags.

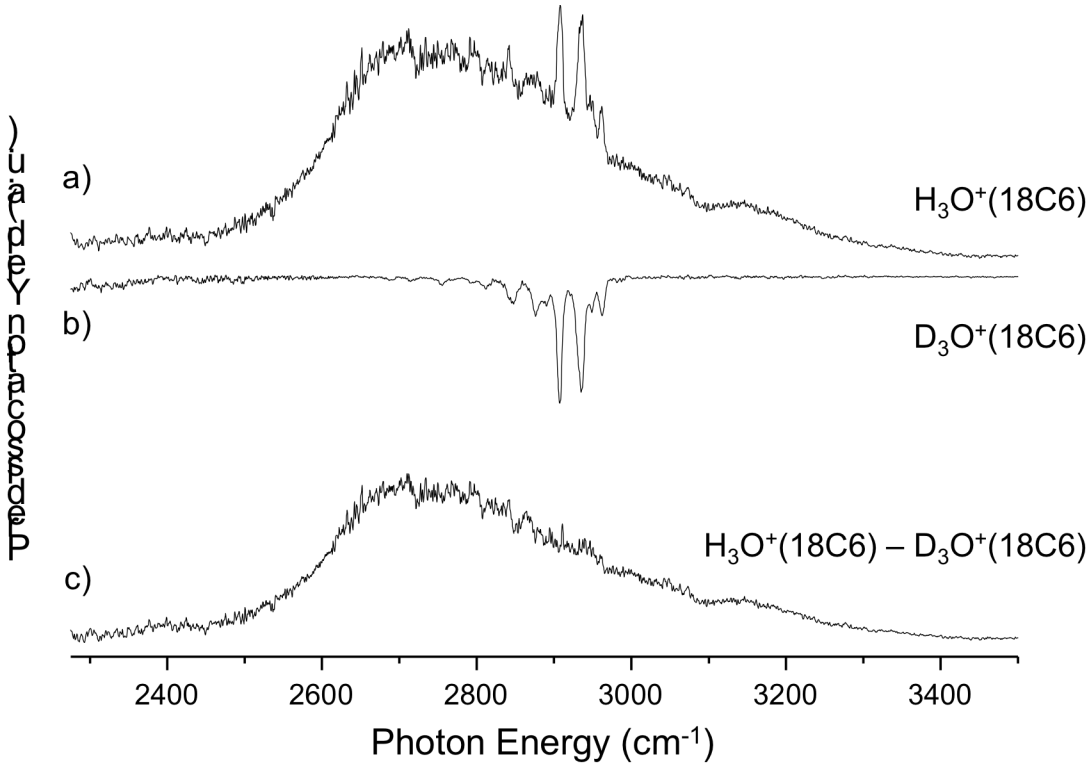


**Figure S3.** Subtraction of b) $D_3O^+$(18C6) from a) $H_3O^+$(18C6) yields the spectrum displayed in trace c) which shows that the removal of the sharp CH peaks from $H_3O^+$(18C6) reveal a homogeneous OH stretching envelope.

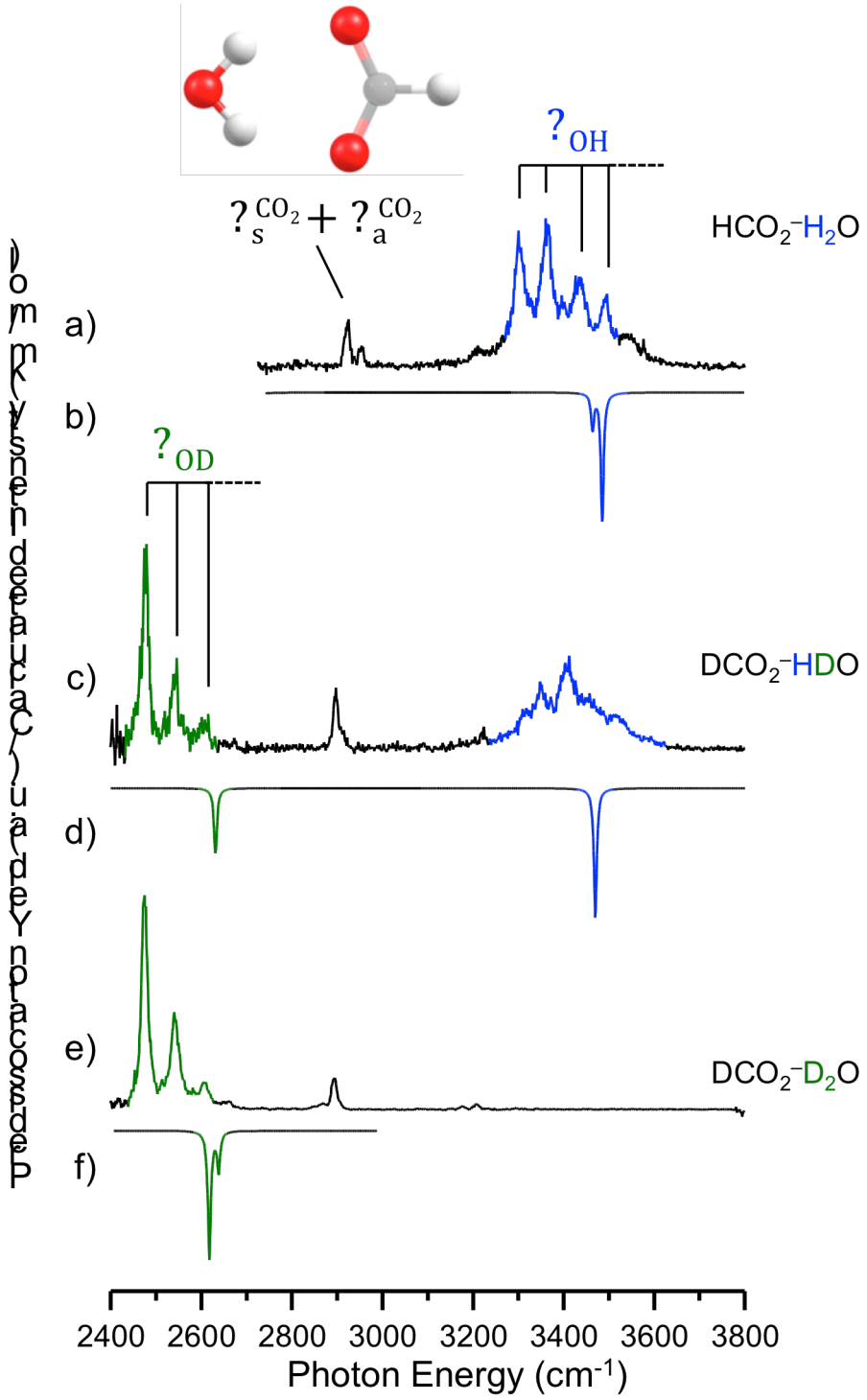


**Figure S4.** Vibrational predissociation spectra of a) $HCO_2^-H_2O$, c) $DCO_2^-HDO$ and e) $DCO_2^-D_2O$ reveal that the OD progression is recovered by a single OD oscillator and the breadth of the OH envelope is recovered by a single OH oscillator. Harmonic calculations (B3LYP/6-311++G(2d,2p) scaled by 0.99556 below 2700 $cm^{-1}$ and by 0.95732 above 2700 $cm^{-1}$) are included as inverted traces in b), d), and f) for each vibrational spectrum.

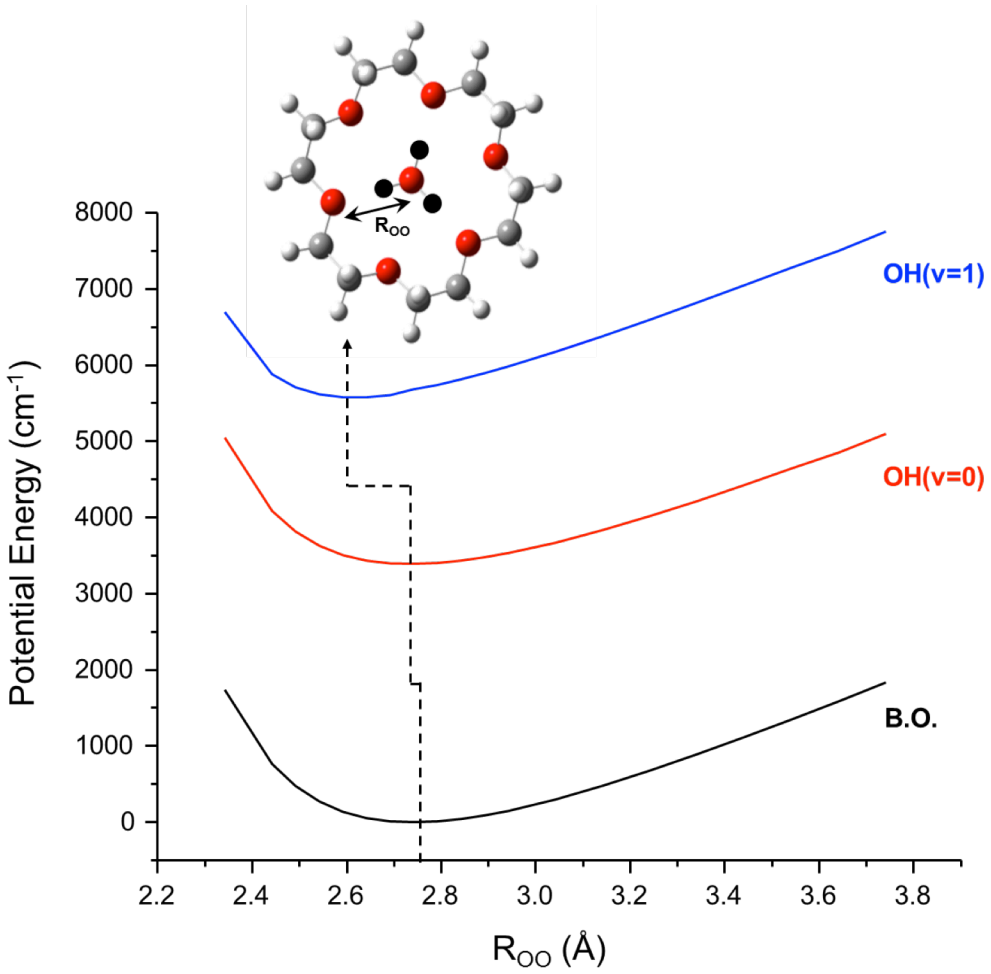


**Figure S5.** Vibrationally adiabatic curves for $D_3O^+$(18C6) as the distance between the oxygen of the central hydronium and the oxygen of the crown ether is scanned (while all other parameters are allowed to relax) for the v=0 and v=1 vibrational levels, obtained by adding the energies of the OD stretch at each position to the Born-Oppenheimer (B.O.) curve. These curves were calculated at the B3LYP/6-311++G(2d,2p) level of theory. The black balls in the structure at the top of the figure indicate deuterons.

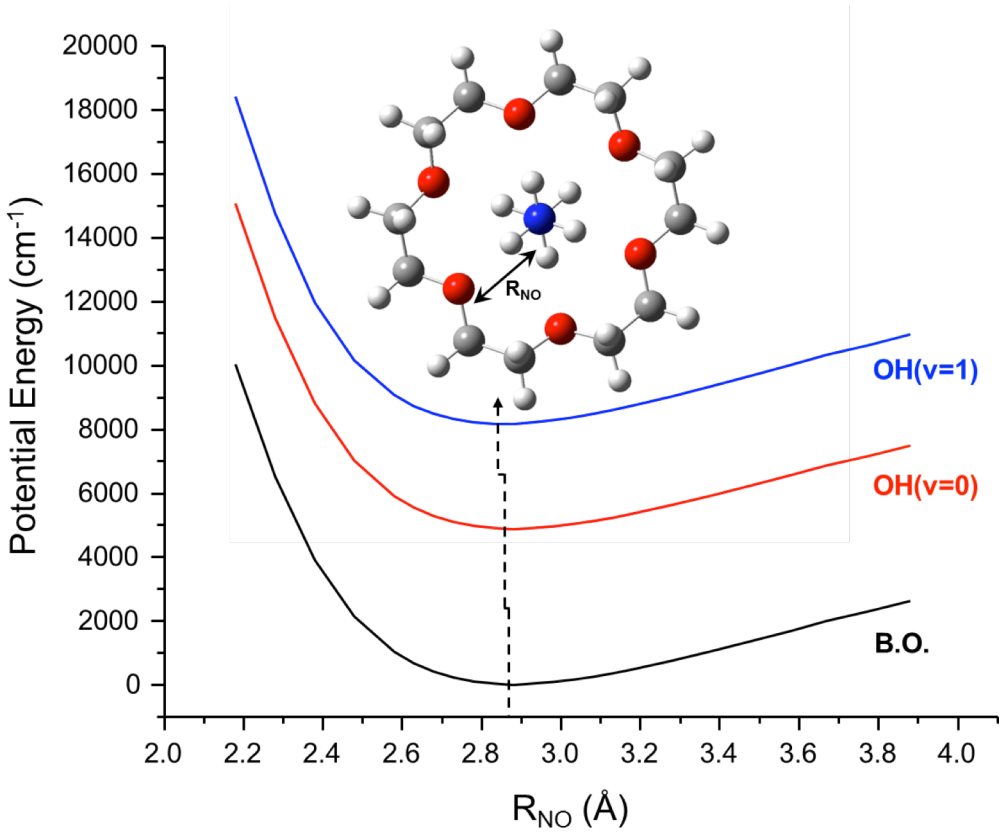


**Figure S6.** Vibrationally adiabatic curves for $CH_3NH_3^+$(18C6) as the distance between the nitrogen of the central ion and the oxygen of the crown ether is scanned (while all other parameters are allowed to relax) for the v=0 and v=1 vibrational levels, obtained by adding the energies of the NH stretch at each position to the Born-Oppenheimer (B.O.) curve. These curves were calculated at the B3LYP/6-311++G(2d,2p) level of theory.

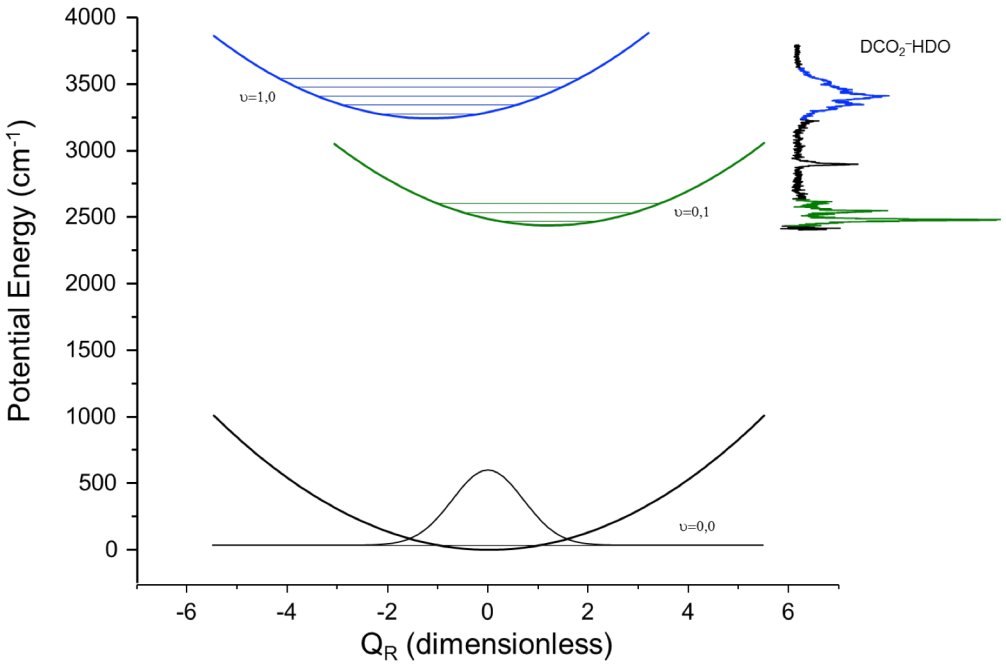


**Figure S7.** Adiabatic rock potential energy curves for $DCO_2^-HDO$ with one quantum of OH stretch using the vibrational adiabatic treatment described later in the SI.

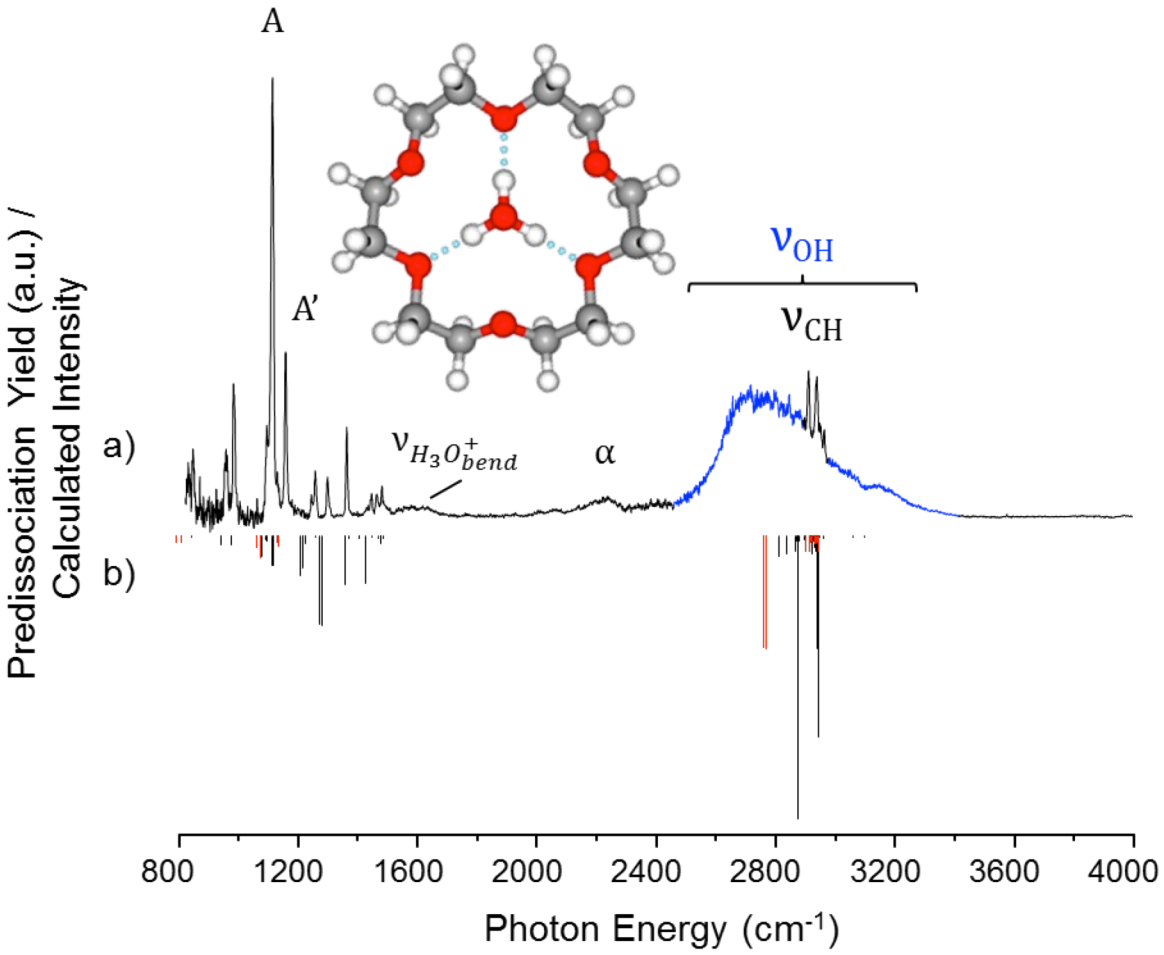


**Figure S8.** Comparison of the $D_2$-tagged predissociation vibrational spectrum of $H_3O^+$(18C6) (a) with anharmonic VPT2 analysis (b) done at the B3LYP/6-311++G(2d,2p) level of theory. Note that the red bars in (b) denote the fundamentals, which have harmonic intensities while the black bars are the anharmonic contributions, which have anharmonic intensities.

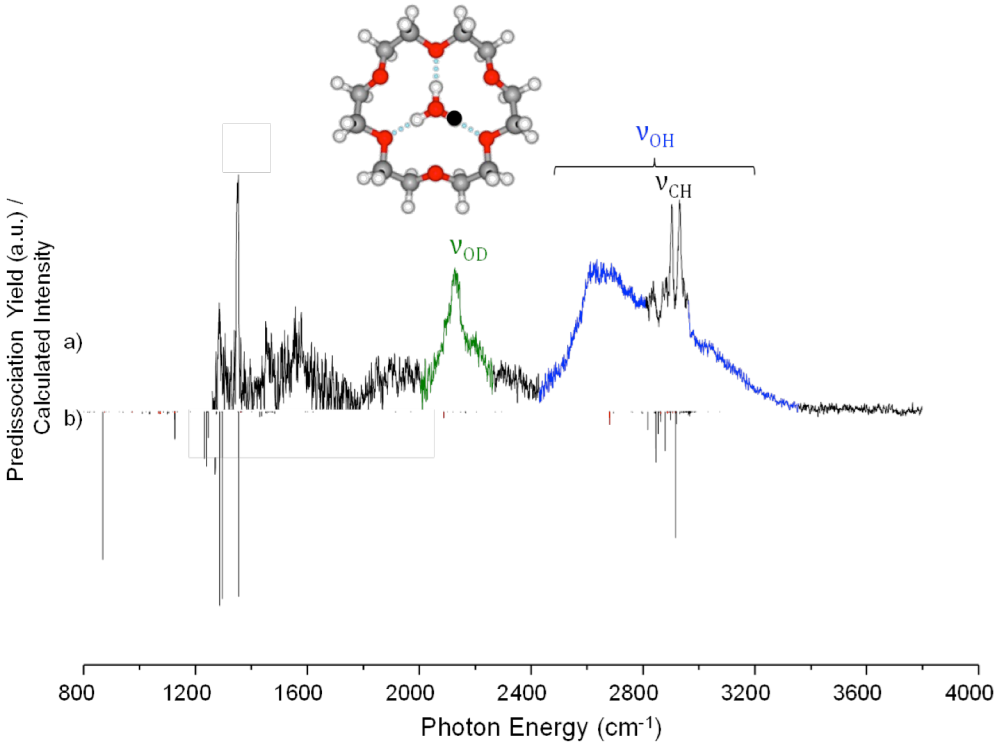


**Figure S9.** Comparison of the $D_2$-tagged predissociation vibrational spectrum of $H_2DO^+$(18C6) (a) with anharmonic VPT2 analysis (b) done at the B3LYP/6-311++G(2d,2p) level of theory. Note that the red bars in (b) denote the fundamentals, which have harmonic intensities while the black bars are the anharmonic contributions, which have anharmonic intensities.

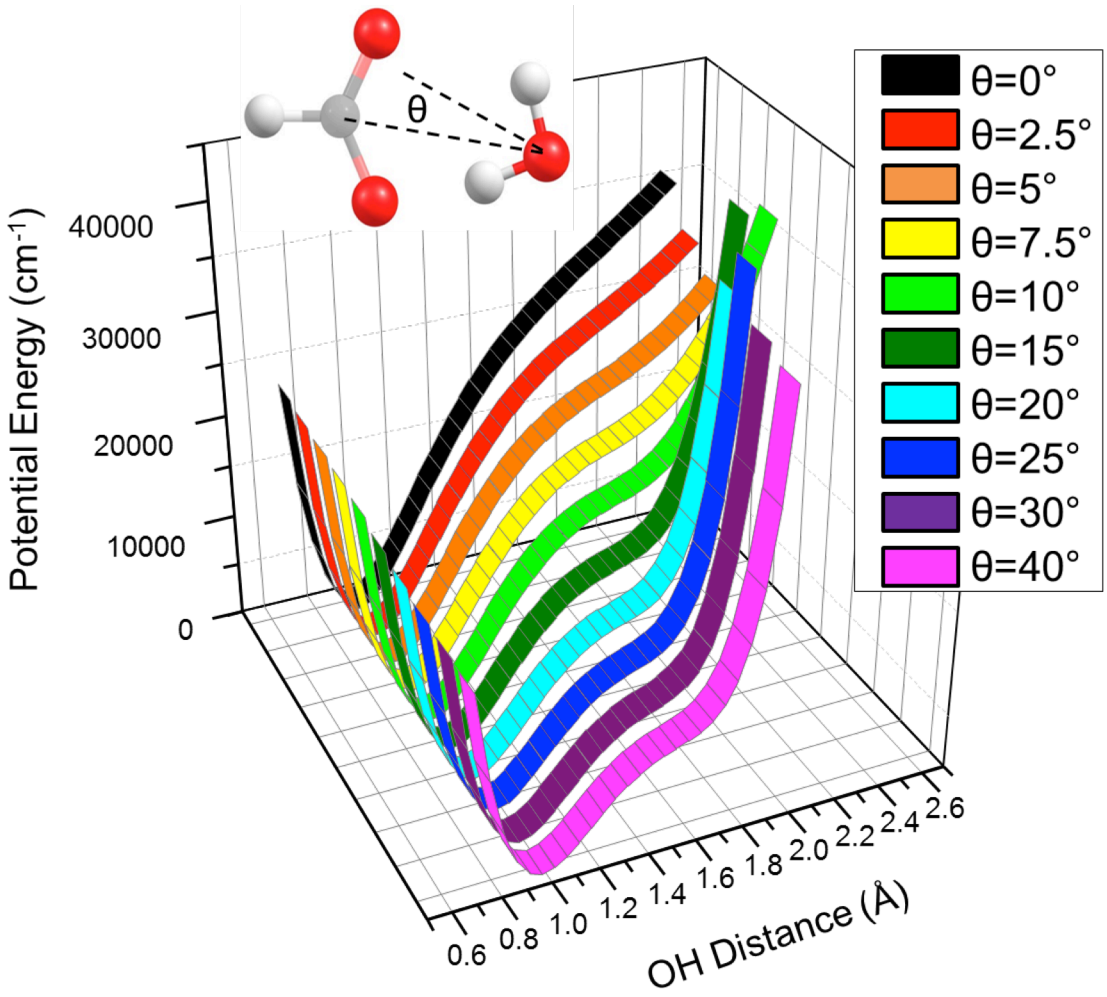


**Figure S10.** Potential energy scans of the OH stretch at various angles of the formate monohydrate rock fundamental show that the shelf potential drops in energy as the tilt angle is increased. All coordinates were held rigid at each angle, except for the shuttling proton. Harmonic calculations were performed at the B3LYP/6-311++G(2d,2p) level of theory.

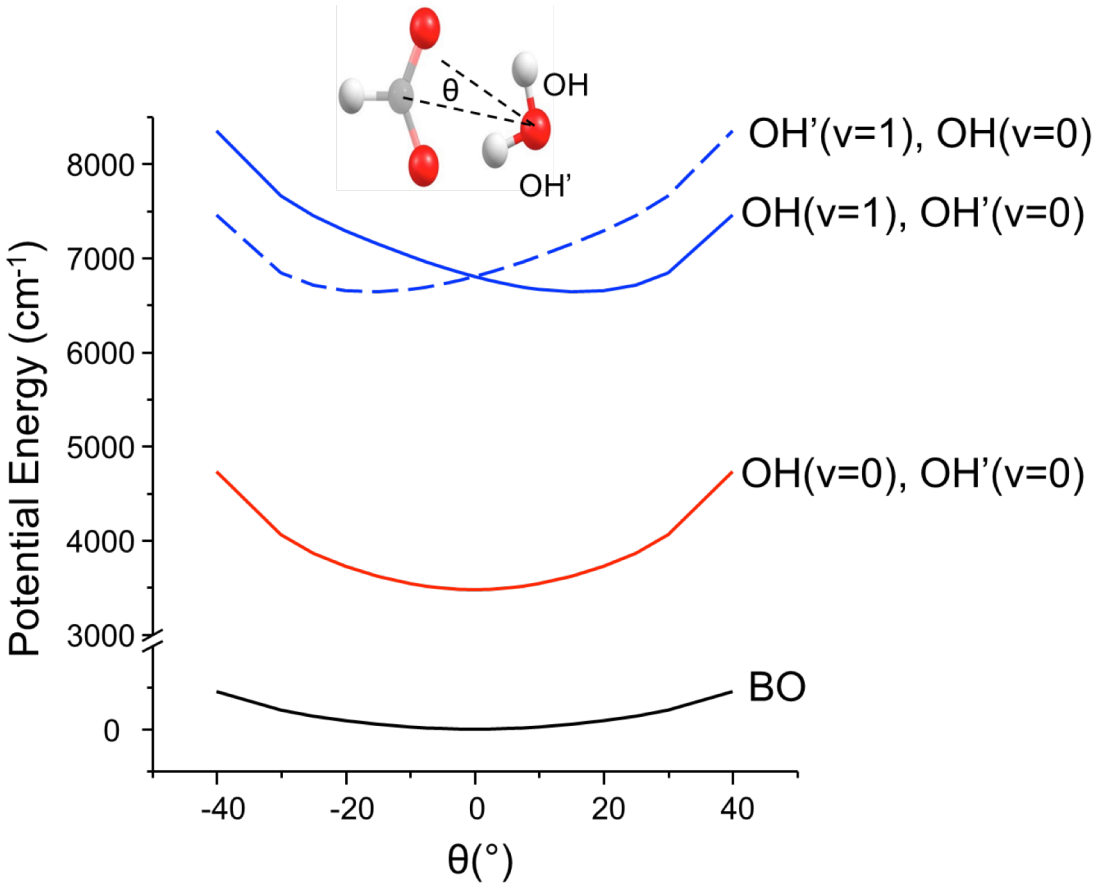


**Figure S11.** Vibrationally adiabatic potential curves for $HCO_2^-$ $H_2O$ obtained from a relaxed scan over the intermolecular the rock angle coordinate (θ) as described in the text. The electronic energies were calculated at the B3LYP/6-311G(2d,2p) level of theory.

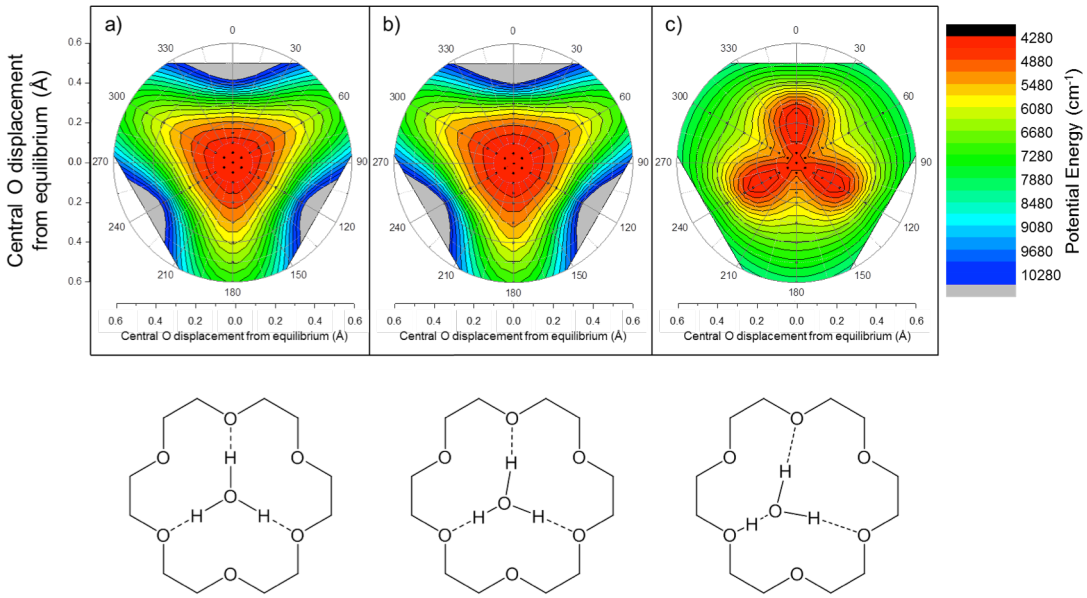


**Figure S12.** Extrapolations of the VA curves similar to that of Fig. 8 in order to mimic the 2D surfaces of $H_3O^+$(18C6) in the a) Born-Oppenheimer (B.O.) surface, and the vibrationally adiabatic surfaces corresponding to b) OH(v=0) and c) OH(v=1). Beneath each surface is a schematic diagram highlighting the distortion of the $H_3O^+$ within the crown upon the addition of each quanta of the OH stretch.

**Table S1:** Intramolecular distances (in Angstroms) in 18-Crown-6 and its guest ion complexes (cf. Fig. 3 for definitions), and their binding energies calculated at the B3LYP/6-311++G(2d,2p) level of theory.

| guest | $r_{OO} = O_1\text{-}O_3$ distance / Å | $r'_{OO} = O_2\text{-}O_4$ distance / Å | $\delta = r_2\text{-}r_1$ / Å | $r_{XO\ X = K, N, O}$ distance / Å | ΔA-A' / $cm^{-1}$ | Binding E / kcal/mol |
|---|---|---|---|---|---|---|
| bare | 5.027 | 5.024 | -0.003 | NA | NA | NA |
| $K^+$ | 4.868 | 4.867 | 0.001 | 2.815 | NA | -65.97 |
| $CH_3NH_3^+$ | 4.804 | 5.038 | 0.235 | 2.890 | 29 | -57.42 |
| $H_3O^+$ | 4.656 | 4.992 | 0.336 | 2.741 | 47 | -88.83 |

**Table S2a:** DFT derived frequencies and scaled frequencies (scaled by 0.99556 below 2700 $cm^{-1}$ and by 0.95732 above 2700 $cm^{-1}$) for the vibrational motions of the guest within 18-Crown-6 performed at the B3LYP/6-311++G(2d,2p) level of theory. Modes localized on the crown ether are omitted for clarity.

| $CH_3NH_3^+$ | | | $H_3O^+$ | | |
|---|---|---|---|---|---|
| ***frequency ($cm^{-1}$)*** | ***scaled frequency ($cm^{-1}$)*** | ***motion*** | ***frequency ($cm^{-1}$)*** | ***scaled frequency ($cm^{-1}$)*** | ***motion*** |
| 87.06 | 86.67 | $CH_3$ rocking | 205.48 | 204.57 | translation |
| 89.66 | 89.26 | $CH_3$ rocking | 206.09 | 205.17 | translation |
| 222.45 | 221.46 | hindered $CH_3$ rotation | 693.02 | 689.94 | twisting |
| 236.57 | 235.52 | rocking | 808.74 | 805.15 | rocking |
| 238.56 | 237.50 | rocking | 814.31 | 810.69 | rocking |
| 271.52 | 270.31 | $NH_3$ translation | 1002.99 | 998.54 | umbrella |
| 272.53 | 271.32 | $NH_3$ translation | 1685.14 | 1677.66 | bend |
| 272.75 | 271.54 | $NH_3$ translation | 1686.50 | 1679.01 | bend |
| 519.2 | 516.89 | twisting | 3081.69 | 2950.16 | asym stretch |
| 541.2 | 538.80 | twisting | 3083.05 | 2951.47 | asym stretch |
| 100.97 | 100.52 | bend | 3134.53 | 3000.75 | sym stretch |
| 1001.4 | 996.95 | bend | | | |
| 1011.9 | 1007.41 | CN stretch | | | |
| 1335.15 | 1329.22 | bend | | | |
| 1338.61 | 1332.67 | bend | | | |
| 1455.75 | 1449.29 | methyl umbrella | | | |
| 1522.25 | 1515.49 | methyl bend | | | |
| 1523.9 | 1517.13 | methyl bend | | | |
| 1619.91 | 1612.72 | ammonia umbrella | | | |
| 1698.78 | 1691.24 | ammonia bend | | | |
| 1700.7 | 1693.15 | ammonia bend | | | |
| 3083.74 | 2952.13 | methyl sym stretch | | | |
| 3166.93 | 3031.77 | methyl asym stretch | | | |
| 3168.14 | 3032.92 | methyl asym stretch | | | |
| 3250.32 | 3111.60 | ammonia sym stretch | | | |
| 3268.24 | 3128.75 | ammonia asym stretch | | | |
| 3269.68 | 3130.13 | ammonia asym stretch | | | |

**Table S2b:** DFT derived frequencies and scaled frequencies (scaled by 0.99556) for the low energy vibrational motions of 18-Crown-6 with $CH_3NH_3^+$ and $H_3O^+$ performed at the B3LYP/6-311++g(2d,2p) level of theory.

| **$CH_3NH_3^+$** | | | **$H_3O^+$** | | |
|---|---|---|---|---|---|
| *frequency ($cm^{-1}$)* | *scaled frequency ($cm^{-1}$)* | *motion* | *frequency ($cm^{-1}$)* | *scaled frequency ($cm^{-1}$)* | *motion* |
| 42.73 | 42.54 | ring wagging | 28.07 | 27.95 | ring wagging |
| 46.14 | 45.94 | ring wagging | 31.59 | 31.45 | ring wagging |
| 65.84 | 65.55 | $CH_3NH_3^+$ out of ring plane | 59.31 | 59.05 | ring wagging |
| 74.35 | 74.02 | ring wagging | 91.47 | 91.06 | $H_3O^+$ out of ring plane |
| 87.06 | 86.67 | $CH_3$ rocking | 92.44 | 92.03 | asym. ring deformation |
| 89.66 | 89.26 | $CH_3$ rocking | 94.49 | 94.07 | asym. ring deformation |
| 106.11 | 105.64 | asym. ring deformation | 135.70 | 135.10 | sym. breathing |
| 107.19 | 106.71 | asym. ring deformation | 147.50 | 146.85 | asym. breathing |
| 149.93 | 149.26 | hindered $CH_3NH_3^+$ rotation | 148.39 | 147.73 | asym. breathing |
| 150.34 | 149.67 | hindered $CH_3NH_3^+$ rotation | 149.95 | 149.28 | asym. breathing |
| 152.00 | 151.33 | asym. ring deformation | 150.65 | 149.98 | asym. breathing |
| 152.78 | 152.10 | asym. ring deformation | 157.35 | 156.65 | hindered $H_3O^+$ rotation |
| 153.76 | 153.08 | asym. ring deformation | 164.22 | 163.49 | $H_3O^+$ out of ring plane |
| 162.55 | 161.83 | asym. ring deformation | 205.48 | 204.57 | translation |
| 163.15 | 162.43 | asym. ring deformation | 206.09 | 205.17 | translation |
| 221.71 | 220.73 | sym. ring deformation | 218.00 | 217.03 | asym. breathing |
| 222.45 | 221.46 | hindered $CH_3$ rotation | 238.12 | 237.06 | asym. breathing |
| 236.57 | 235.52 | rocking | 238.57 | 237.51 | ring deformation |
| 238.56 | 237.50 | rocking | 265.64 | 264.46 | sym. breathing |
| 240.51 | 239.44 | rocking | 279.27 | 278.03 | ring deformation |
| 240.90 | 239.83 | sym. ring deformation | 280.75 | 279.50 | ring deformation |
| 255.18 | 254.05 | sym. breathing | 287.62 | 286.34 | ring deformation |
| 271.52 | 270.31 | $NH_3^+$ translation | 319.03 | 317.61 | ring deformation |
| 272.53 | 271.32 | $NH_3^+$ translation | 319.19 | 317.77 | ring deformation |

| | | | | | |
|---|---|---|---|---|---|
| 272.75 | 271.54 | $NH_3^+$ translation | 345.64 | 344.11 | ring deformation |
| 320.61 | 319.19 | $NH_3^+$ translation | 362.75 | 361.14 | ring deformation |
| 320.82 | 319.40 | $NH_3^+$ translation | 363.48 | 361.87 | ring deformation |
| 347.51 | 345.97 | asym. ring deformation | | | |
| 358.69 | 357.10 | asym. ring deformation | | | |
| 359.38 | 357.78 | asym. ring deformation | | | |

## II. Experimental and computational details

*Tag-free spectrum of $D_3O^+(D_2O)_3$*

Two-color (IR-IR) double resonance measurements were carried out by applying two laser pulses to the same mass selected ion packet at two different laser interaction regions. The first laser is scanned while the second laser is held at a vibrational transition (2774 $cm^{-1}$) unique to the "warm" $D_3O^+(D_2O)_3$ cluster produced by excitation throughout the scan range 1800-2200 $cm^{-1}$. This enables enhanced photofragmentation of the strongly bound, cryogenically cooled cluster upon resonant absorption of a single photon at the first laser interaction thus revealing the linear spectrum without requiring a weakly bound tag.

*Computational details:*

Starting structures were selected according to Oomens et al.[1] and optimized at the B3LYP/6-311++G(2d,2p) level of theory using the Bernie algorithm within the Gaussian G09 software package. Harmonic frequency calculations on the resulting structures were checked for imaginary frequencies. Binding energies of cations $K^+$, $H_3O^+$ and $CH_3NH_3^+$ were corrected for basis set superposition errors and zero point energies. Two scaling factors were applied for comparison of theoretical predicted vibrational spectra to experimental data. A set of scaling factors was derived for the CO stretching motion from all complexes under study and averaged, resulting in 0.9956(4). The CH stretching region was scaled with respect to the most blue shifted CH bands, resulting in an averaged scaling factor of 0.9573(5).

The vibrationally adiabatic scans were performed using the B3LYP/6-311++G(2d,2p) level of theory by varying the distance between the central oxygen/nitrogen of the $H_3O^+/CH_3NH_3^+$ and allowing all other parameters to relax. The OH(v=0) and OH(v=1) curves were found by adding 0.5 and 1.5 quanta of the OH/NH stretches.

The barrier between the two isomers of the $H_3O^+$(18C6) was calculated through a comparison of the minimum energy structure with that of the transition state structure, where the transition state is the frustrated rotation between the two isomers.

*Vibrationally adiabatic model for formate monohydrate details* :

Following the discussion of Sibert and co-workers,[2] we perform an adiabatic treatment of the three-dimensional potential model for formate monohydrate. This model focuses on harmonic treatments of the two local OH/OD stretches, $Q_1$ and $Q_2$, and the rock, $Q_R$, along with a cubic coupling term that is quadratic in the OH stretch and linear in the rock coordinate:

$$V_{cubic}(Q_1, Q_2, Q_R) = \frac{F_{ssr}}{2}(Q_1^2 + Q_2^2)Q_R \qquad \text{(Eq S1)}$$

Analysis of this model using dimensionless normal modes (e.g. force constants in units of $cm^{-1}$ and the associate normal coordinates containing no physical dimensions) yields the following expressions:

Transition frequencies:

$$E(v_{\mathrm{OH}} = 1, n_{rock}) = \nu_{\mathrm{OH/D}} + n_{\mathrm{rock}}\nu_{\mathrm{rock}} - E_{\mathrm{shift}} \qquad \text{(Eq S2)}$$

where

$$\mathrm{E_{shift}} = -\frac{F_{ssr}^2}{8\nu_{\mathrm{rock}}} \qquad \text{(Eq S3)}$$

is the shift between the first peak in the progression and the anharmonic OH stretch frequency. Likewise the intensities are given by

$$I(n_{rock}) = e^{-\left(\frac{\Delta Q_R^2}{2}\right)} \frac{\Delta Q_R^{2n_{\mathrm{rock}}}}{2^{n_{\mathrm{rock}}}(n_{\mathrm{rock}})!} \qquad \text{(Eq S4)}$$

where

$$\Delta Q_R = \pm\frac{F_{ssr}}{2\nu_{\mathrm{rock}}} \qquad \text{(Eq S5)}$$

represents the shift in the minimum of the harmonic potential in the rock coordinate with OH stretch excitation.

The parameters used for this treatment were obtained by analyzing the spectra of these complexes. Based on this analysis, the average spacing (rock frequency, $\nu_{\mathrm{rock}}$) was found to be 67 $cm^{-1}$ for both the HOH and DOD complexes. The origin of the HOH band was at 3298 $cm^{-1}$ while the origin in the DOD band was at 2474 $cm^{-1}$. These values correspond to anharmonic OH and OD frequencies, $\nu_{\mathrm{OH/D}}$ of 3414.6 and 2532.3 $cm^{-1}$, respectively. Finally the coefficient of the cubic coupling $F_{ssr}$ was taken to be 195 $cm^{-1}$ for the HOH complex and scaled by $1/\sqrt{2}$ for

the DOD complex. This value was chosen to optimally reproduce the intensity pattern in the recorded spectrum.

In addition, for comparison, one-dimensional cuts through the potential surface for the formate monohydrate complex were evaluated at the B3LYP/6-311++G(2d,2p) level of theory and basis set. These curves were evaluated by first adjusting the angle between the biscector of the HOH angle and the vector that connects the oxygen in water to the carbon atom in formate. In these scans all other coordinates are allowed to relax. Based on this one-dimensional potential curve, this angle, θ≈ 10 $Q_R$. Using these optimized geometries, one-dimensional cuts of the potential surface were evaluated as functions of the extension and compression of a single OH bond length. The resulting curves are shown in Figure S10. With these curves in hand the v=0 and 1 energies of the OH stretch were evaluated for each value of θ using a Discrete Variable Representation[3] where $r_{OH}$ varied from 0.5 Å to 2.5 Å, and 200 grid points were used for the calculation. Because all of the other atoms were constrained in the scan, the mass of hydrogen, 1.007825 amu, was used for this calculation. The resulting calculated adiabatic potential curves (electronic energy plus the sum of the energy in the two OH oscillators) for formate monohydrate are plotted in Figure S11. As can be seen, these are similar to the curves obtained using the simple model potential, described above, thereby providing additional confidence in this approximation.

*Seven mode coupling details:*

Based on the discussion of the vibrationally adiabatic treatment of the formate monohydrate system, one way to rationalize the breadth of the OH stretch feature and the structure in the OD stretch feature of the $H_3O^+$(18C6) complexes is through a similar model. As we consider the low-frequency modes in these complexes that could be strongly coupled to the OH/OD stretches, by analogy to the rocking motion in formate monohydrate, two such vibrations emerge. Both are doubly degenerate in $C_3$ symmetry, and are illustrated in Figure S13. Following this model in which there are now three high-frequency vibrations, $\nu_{OH,1}$, $\nu_{OH,2}$ and $\nu_{OH,3}$, and four low-frequency modes, $\nu_{1,a}$, $\nu_{1,b}$, $\nu_{2,a}$ and $\nu_{2,b}$, we set up a model Hamiltonian that includes couplings between the three OH/D stretch fundamentals and combination bands including one quantum of OH/D stretch and multiple quanta in the combinations of the four low-frequency vibrations. Specifically,

$$H_{7d} = \sum_{i=1}^{3}\left\{\nu_{\mathrm{H},i} + \frac{1}{\sqrt{8}}\sum_{j=1}^{2}\left[F_{iij_a}\left(a_{j_a}^{+} + a_{j_a}^{-}\right) + F_{iij_b}\left(a_{j_b}^{+} + a_{j_b}^{-}\right)\right]\right\}\left(\hat{n}_i + \frac{1}{2}\right) + \sum_{j=1}^{2}\nu_i\,\hat{n}_j + \sum_{i=1}^{3}\sum_{j=1}^{i-1}\frac{1}{\sqrt{8}}\left\{\sum_{k=1}^{2}F_{ijk_a}\left(a_{\mathrm{H},i}^{+}a_{\mathrm{H},j}^{-} + a_{\mathrm{H},i}^{-}a_{\mathrm{H},j}^{+}\right)\left(a_{k_a}^{+} + a_{k_a}^{-}\right) + \sum_{k=1}^{2}F_{ijk_b}\left(a_{\mathrm{H},i}^{+}a_{\mathrm{H},j}^{-} + a_{\mathrm{H},i}^{-}a_{\mathrm{H},j}^{+}\right)\left(a_{k_b}^{+} + a_{k_b}^{-}\right)\right\} \quad \text{(Eq S6)}$$

Here, $a^{+/-}$ represent harmonic oscillator raising and lowering operators, and $\hat{n}_i = a_i^{+}a_i^{-}$ is the number operator. Within this representation, a basis contains one quantum in one of the OH/D

oscillators, and up to 2000 $cm^{-1}$ of energy distributed among the low-frequency modes. This corresponds to roughly 8000 states in the basis.

The Hamiltonian matrix is diagonalized and the intensity is determined based on the harmonic transition moments for the three OH/D stretches. The parameters used for the reported calculations on $H_3O^+$ and $H_2DO^+$ are provided in Tables S3a and S3b.

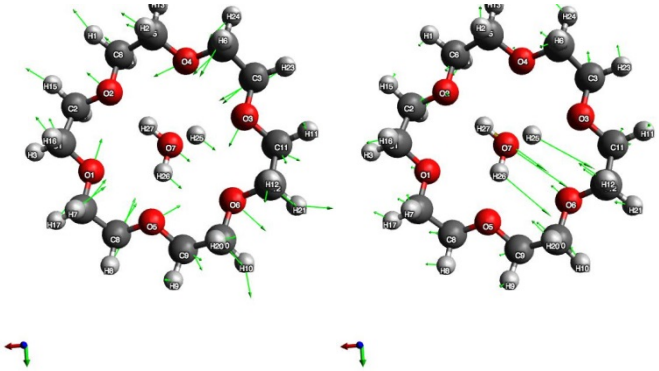

**Figure S13**: Illustrations of the two low-frequency modes used in the seven-dimensional model Hamiltonian. The mode on the left (mode 2) has a frequency of 92.4/94.5 $cm^{-1}$ (unscaled) and corresponds to primarily ring breathing with some contribution from the $H_3O^+$ translation within the cage. The mode on the right (mode 1) has a frequency of 205.5/206.1 $cm^{-1}$ (unscaled) and corresponds to primarily $H_3O^+$ translation with some contribution from ring breathing. Both modes are nearly doubly degenerate, and would correspond to the two components of an E vibration if the cluster had perfect $C_3$ symmetry.

**Table S3a**. Parameters for the Hamiltonian in Eq. S6. The frequencies for the OH/D stretches are the anharmonic frequencies obtained using VPT2 at the B3LYP/6-311++G(2d,2p) level of theory/basis as implemented in Gaussian 09.[4] The frequencies for the low-frequency modes are the harmonic frequencies obtained at the same level of theory. As described in the text, the remaining terms are the cubic force constants obtained from the VPT2 calculation. All parameters are provided in $cm^{-1}$.

| Term | $H_3O^+$ | $H_2DO^+$ |
|---|---|---|
| $\nu_{H,1}$ | 2802.938 | 2683.116 |
| $\nu_{H,1}$ | 2762.038 | 2684.245 |
| $\nu_{H,1}$ | 2752.247 | 2088.625 |
| $\nu_{1,a/b}$ | 206.086/205.475 | 200.228/197.824 |
| $\nu_{2,a/b}$ | 94.494/92.440 | 91.635/90.689 |
| $F_{H,1;H,1,1a/b}$ | -5.64668/-4.23569 | 61.12629/-30.05620 |
| $F_{H,1;H,1,2a/b}$ | 3.60580/1.56022 | 48.96819/25.11424 |
| $F_{H,1;H,2,1a/b}$ | 97.48011/-138.33505 | 106.35174/-114.49091 |
| $F_{H,1;H,2,2a/b}$ | 106.75285/89.32426 | 9.90553/-197.79928 |
| $F_{H,1;H,3,1a/b}$ | -132.13050/-97.16401 | -3.36146/-9.22439 |
| $F_{H,1;H,3,2a/b}$ | 85.81034/-100.50475 | -9.18318/2.25066 |
| $F_{H,2;H,2,1a/b}$ | -10.77828/-124.75026 | 57.26913/-11.02760 |
| $F_{H,2;H,2,2a/b}$ | 103.73598/11.48406 | 52.60405/54.55815 |
| $F_{H,2;H,3,1a/b}$ | 125.27887/1.14416 | -7.18742/7.17459 |
| $F_{H,2;H,3,2a/b}$ | -8.05593/105.08159 | 0.00000/10.05962 |
| $F_{H,3;H,3,1a/b}$ | -0.70944/132.24220 | -58.59851/66.14655 |
| $F_{H,3;H,3,2a/b}$ | -111.32965/0.63847 | 43.49492/-56.25007 |

**Table S3b**. Harmonic transition moments for the OH stretches. These have been normalized so their squared magnitude is the harmonic intensity in km $mol^{-1}$.

| Vibration | Coordinate | $H_3O^+$ | $H_2DO^+$ |
|---|---|---|---|
| $H_1$ | *x* | -54.758 | 26.694 |
| | *y* | 3.704 | -27.227 |
| | *z* | 0.147 | 2.906 |
| $H_2$ | *x* | 3.577 | 39.858 |
| | *y* | 55.229 | 37.530 |
| | *z* | -0.096 | -0.274 |
| $H_3$ | *x* | 0.767 | -23.375 |
| | *y* | 0.601 | 26.631 |
| | *z* | 8.605 | 7.271 |

*Sample preparation:*

**Preparation of 18C6 stock solution.** 2.6 mg (9.84 mmol) of 18C6 was diluted with water (1 mL) and acetonitrile (7 mL) and then sonicated for 5 minutes to prepare a 1.23 mM solution of 18C6.

**Synthesis of [$H_3O^+$(18C6)].** 0.16 mL (0.16mmol) of 1M $H_2SO_4$ was directly added to 2.6 mg (9.84 mmol) of 18C6. This solution was then diluted with water (0.64 mL) and acetonitrile (7.2 mL) and then sonicated for 5 minutes to create a 0.02 mM solution of $H_3O^+$(18C6). In order to prepare $D_3O^+$(18C6), the samples were instead made using $D_2SO_4$ and $D_2O$.

**Synthesis of [$K^+$(18C6)].** A 1.25 mM solution of $K^+$ was prepared with 1.66 mg (10.0 mmol) of KI in water (1 mL) and acetonitrile (7 mL) and then sonicated for 5 minutes. Then an equivolume amount of the 1.25 mM $K^+$ solution was added to the 1.23 mM 18C6 stock solution and sonicated again for 5 minutes.

**Synthesis of [$CH_3NH_3^+$(18C6)].** 0.3 mL (0.3 mmol) of 1M $H_2SO_4$ was directly added to 0.4 mL (12.9 mmol) of $CH_3NH_2$. This solution was then diluted with water (0.6 mL) and acetonitrile (7.1 mL) and then sonicated for 5 minutes to create a 0.038 mM solution of $CH_3NH_3^+$(18C6). Then an equivolume amount of the 0.0338 mM $CH_3NH_3^+$ solution was added to the 1.23 mM 18C6 stock solution and sonicated again for 5 minutes.

Partial H/D exchange for the $H_3O^+$(18C6) complex was achieved by performing electrospray under a $D_2O$ atmosphere.

*DFT input coordinates:*

**Table S4a:** XYZ coordinates of the geometry optimized cations $K^+$(18C6) and $CH_3NH_3^+$(18C6) at the B3LYP level of theory using the 6-311++G(2d,2p) (H, C, N, O, K) basis set (charge +1, multiplicity=1).

| $K^+$(18C6) | | | | $CH_3NH_3^+$(18C6) | | | |
|---|---|---|---|---|---|---|---|
| C | -3.614943 | 0.462754 | 0.297966 | C | -3.638983 | 0.226444 | -0.481157 |
| C | -3.180747 | 1.778499 | -0.298197 | C | -3.300132 | 1.571132 | 0.116047 |
| C | -3.130750 | -1.865380 | 0.298392 | C | -3.005935 | -2.060766 | -0.486809 |
| C | -2.208200 | -2.899094 | -0.297903 | C | -2.025952 | -3.043501 | 0.107929 |
| C | -1.406640 | 3.361777 | -0.297913 | C | -1.622470 | 3.277676 | 0.105257 |
| C | -0.050125 | 3.643837 | 0.298238 | C | -0.282474 | 3.631625 | -0.493933 |
| C | 0.050129 | -3.643836 | -0.298217 | C | 0.290200 | -3.644193 | 0.105122 |
| C | 1.406651 | -3.361782 | 0.297924 | C | 1.623712 | -3.261781 | -0.490845 |
| C | 2.208201 | 2.899090 | 0.297971 | C | 2.015479 | 3.036988 | -0.487176 |
| C | 3.130763 | 1.865386 | -0.298321 | C | 3.010634 | 2.073905 | 0.114497 |
| C | 3.180750 | -1.778500 | 0.298217 | C | 3.290183 | -1.571305 | -0.483953 |
| C | 3.614941 | -0.462749 | -0.297938 | C | 3.648208 | -0.232943 | 0.116582 |
| H | -4.646465 | 0.259196 | -0.007421 | H | -4.692831 | 0.006091 | -0.277677 |
| H | -4.158019 | -2.089916 | -0.006609 | H | -4.023897 | -2.413326 | -0.286721 |
| H | -3.889107 | 2.555848 | 0.006262 | H | -4.016405 | 2.310560 | -0.254519 |
| H | -3.583961 | 0.514020 | 1.391463 | H | -3.497878 | 0.257746 | -1.566645 |
| H | -3.185280 | 1.718487 | -1.391691 | H | -3.375637 | 1.536508 | 1.207707 |
| H | -3.081556 | -1.899750 | 1.391872 | H | -2.867091 | -2.010385 | -1.571845 |
| H | -2.547615 | -3.894310 | 0.007191 | H | -2.372558 | 3.979578 | -0.271313 |
| H | -2.237042 | -2.846402 | -1.391398 | H | -2.259870 | -4.044136 | -0.267748 |
| H | -2.098584 | 4.153693 | 0.006811 | H | -2.111035 | -3.057921 | 1.199409 |
| H | -1.346707 | 3.359885 | -1.391422 | H | -1.588955 | 3.363000 | 1.196241 |
| H | -0.268925 | -4.645828 | 0.006715 | H | -0.311218 | 3.483569 | -1.578556 |
| H | -0.104502 | 3.618513 | 1.391752 | H | -0.077320 | 4.689790 | -0.296863 |
| H | 0.104494 | -3.618492 | -1.391731 | H | 0.007885 | -4.631822 | -0.271626 |
| H | 0.268935 | 4.645821 | -0.006711 | H | 0.359589 | -3.699734 | 1.196370 |
| H | 1.346736 | -3.359930 | 1.391433 | H | 1.526595 | -3.151225 | -1.575960 |
| H | 2.098598 | -4.153679 | -0.006843 | H | 1.973708 | 2.896193 | -1.572323 |
| H | 2.237029 | 2.846392 | 1.391465 | H | 2.341815 | -4.064778 | -0.290465 |
| H | 2.547613 | 3.894311 | -0.007116 | H | 2.349771 | 4.060901 | -0.286185 |
| H | 3.081587 | 1.899771 | -1.391802 | H | 3.015678 | 2.159787 | 1.205997 |
| H | 3.185311 | -1.718506 | 1.391711 | H | 3.183137 | -1.473291 | -1.569331 |
| H | 3.583946 | -0.514005 | -1.391436 | H | 3.695606 | -0.302890 | 1.208203 |
| H | 3.889095 | -2.555849 | -0.006276 | H | 4.009926 | 2.324068 | -0.254241 |
| H | 4.158028 | 2.089921 | 0.006698 | H | 4.103081 | -2.277471 | -0.281160 |
| H | 4.646468 | -0.259198 | 0.007435 | H | 4.634346 | 0.065343 | -0.251636 |
| O | -2.751300 | -0.572166 | -0.168391 | O | -2.804815 | -0.775296 | 0.091428 |

| | | | | | | | |
|---|---|---|---|---|---|---|---|
| O | -1.871284 | 2.096781 | 0.169120 | O | -1.976118 | 1.945036 | -0.275135 |
| O | -0.880143 | -2.668608 | 0.168518 | O | -0.696960 | -2.682556 | -0.278447 |
| O | 0.880151 | 2.668598 | -0.168467 | O | 0.730486 | 2.814997 | 0.084368 |
| O | 1.871271 | -2.096763 | -0.169070 | O | 2.073210 | -2.040581 | 0.087052 |
| O | 2.751307 | 0.572167 | 0.168440 | O | 2.674168 | 0.739041 | -0.273706 |
| K | -0.000015 | -0.000004 | -0.000151 | N | 0.000295 | 0.000131 | 0.537926 |
| | | | | H | -0.686377 | 0.680057 | 0.180316 |
| | | | | H | -0.243807 | -0.934230 | 0.178208 |
| | | | | H | 0.932749 | 0.256670 | 0.182003 |
| | | | | C | -0.002627 | -0.003527 | 2.023575 |
| | | | | H | -0.992969 | -0.276772 | 2.373900 |
| | | | | H | 0.255496 | 0.988780 | 2.379818 |
| | | | | H | 0.727562 | -0.725241 | 2.375858 |

**Table S4b:** XYZ coordinates of the geometry optimized cation $H_3O^+$(18C6) at the B3LYP level of theory using the 6-311++G(2d,2p) (H, C, O) basis set (charge +1, multiplicity=1).

| $H_3O^+$(18C6) | | | |
|---|---|---|---|
| C | -3.597112 | 0.301724 | -0.268603 |
| C | -3.254561 | 1.621118 | 0.367388 |
| C | -3.002964 | -2.001827 | -0.270473 |
| C | -2.066837 | -2.991748 | 0.366717 |
| C | -1.559377 | 3.283763 | 0.372409 |
| C | -0.232160 | 3.602857 | -0.259600 |
| C | 0.221464 | -3.626453 | 0.376874 |
| C | 1.537550 | -3.266794 | -0.256500 |
| C | 2.058789 | 2.964190 | -0.264933 |
| C | 3.032843 | 2.006664 | 0.365275 |
| C | 3.234996 | -1.601106 | -0.268603 |
| C | 3.626954 | -0.292494 | 0.361242 |
| H | -4.573655 | -0.029803 | 0.092471 |
| H | -4.049526 | 2.341979 | 0.146349 |
| H | -4.018627 | -2.183774 | 0.088879 |
| H | -3.638166 | 0.398572 | -1.356886 |
| H | -3.180310 | 1.510935 | 1.454770 |
| H | -2.990197 | -2.105570 | -1.358782 |
| H | -2.414523 | -4.006957 | 0.145473 |
| H | -2.264094 | 4.093103 | 0.151524 |
| H | -2.056052 | -2.859031 | 1.454042 |
| H | -1.454167 | 3.204598 | 1.459895 |
| H | -0.326694 | 3.650379 | -1.347819 |
| H | -0.004175 | -4.676525 | 0.160321 |
| H | 0.117890 | 4.571167 | 0.106053 |
| H | 0.275223 | -3.501390 | 1.463802 |
| H | 1.477669 | -3.357000 | -1.344476 |
| H | 2.160124 | 2.954035 | -1.353503 |
| H | 2.260555 | 3.974725 | 0.098158 |
| H | 2.311526 | -3.944974 | 0.110806 |
| H | 2.903208 | 1.992826 | 1.452927 |
| H | 3.316361 | -1.543540 | -1.357381 |
| H | 3.510244 | -0.344331 | 1.449222 |
| H | 3.900547 | -2.388450 | 0.093257 |
| H | 4.053526 | 2.336997 | 0.142769 |
| H | 4.679565 | -0.087862 | 0.136077 |
| O | -2.604618 | -0.671016 | 0.095694 |
| O | -2.017436 | 2.056797 | -0.171657 |
| O | -0.772389 | -2.776110 | -0.170869 |

| | | | |
|---|---|---|---|
| O | 0.720708 | 2.589821 | 0.100912 |
| O | 1.883575 | -1.918881 | 0.100842 |
| O | 2.792191 | 0.719143 | -0.178146 |
| O | -0.000860 | 0.000255 | -0.432067 |
| H | -0.944129 | -0.242543 | -0.191049 |
| H | 0.260285 | 0.938304 | -0.190518 |
| H | 0.680720 | -0.695293 | -0.191204 |

**Table S4c:** XYZ coordinates of the geometry optimized cations $HCO_2^-H_2O$ the B3LYP level of theory using the 6-311++G(2d,2p) (H, C, O) basis set (charge -1, multiplicity=1).

| $HCO_2^-H_2O$ | | | |
|---|---|---|---|
| C | 0 | 1.144333 | 0 |
| O | -1.13827 | 0.602636 | 0 |
| H | -0.0016 | 2.275833 | 0 |
| O | 1.139551 | 0.605631 | 0 |
| O | 0.000358 | -2.01296 | 0 |
| H | 0.730653 | -1.36115 | 0 |
| H | -0.74219 | -1.34317 | 0 |

## References


1. Hurtado, P.; Gamez, F.; Hamad, S.; Martinez-Haya, B.; Steill, J. D.; Oomens, J. Crown Ether Complexes with $H_3O^+$ and $NH_4^+$: Proton Localization and Proton Bridge Formation. *J. Phys. Chem. A* **2011,** *115* (25), 7275-7282.
2. Myshakin, E. M.; Sibert, E. L., III; Johnson, M. A.; Jordan, K. D. Large anharmonic effects in the infrared spectra of the symmetrical $CH_3NO_2^-\cdot(H_2O)$ and $CH_3CO_2^-\cdot(H_2O)$ complexes. *J. Chem. Phys.* **2003,** *119*, 10138-10145.
3. Colbert, D. T.; Miller, W. H. A novel discrete variable representation for quantum mechanical reactive scattering via the S-matrix Kohn method. *J. Chem. Phys.* **1992,** *96* (3), 1982.
4. Frisch, M. J.; Trucks, G. W.; Schlegel, H. B.; Scuseria, G. E.; Robb, M. A.; Cheeseman, J. R.; Scalmani, G.; Barone, V.; Mennucci, B.; Petersson, G. A.; Nakatsuji, H.; Caricato, M.; Li, X.; Hratchian, H. P.; Izmaylov, A. F.; Bloino, J.; Zheng, G.; Sonnenberg, J. L.; Hada, M.; Ehara, M.; Toyota, K.; Fukuda, R.; Hasegawa, J.; Ishida, M.; Nakajima, T.; Honda, Y.; Kitao, O.; Nakai, H.; Vreven, T.; J. A. Montgomery, J.; Peralta, J. E.; Ogliaro, F.; Bearpark, M.; Heyd, J. J.; Brothers, E.; Kudin, K. N.; Staroverov, V. N.; Kobayashi, R.; Normand, J.; Raghavachari, K.; Rendell, A.; Burant, J. C.; Iyengar, S. S.; Tomasi, J.; Cossi, M.; Rega, N.; Millam, J. M.; Klene, M.; Knox, J. E.; Cross, J. B.; Bakken, V.; Adamo, C.; Jaramillo, J.; Gomperts, R.; Stratmann, R. E.; Yazyev, O.; Austin, A. J.; Cammi, R.; Pomelli, C.; Ochterski, J. W.; Martin, R. L.; Morokuma, K.; Zakrzewski, V. G.; Voth, G. A.; Salvador, P.; Dannenberg, J. J.; Dapprich, S.; Daniels, A. D.; Farkas, Ö.; Foresman, J. B.; Ortiz, J. V.; Cioslowski, J.; Fox, D. J. *Gaussian 09, Revision D.01*, Gaussian, Inc.: Wallingford, CT, 2009.